Determination of water uptake in organic coatings deposited on 2024 aluminium alloy: Comparison between impedance measurements and gravimetry

Anh Son Nguyen, Nicolas Causse, Marco Musiani, Mark E. Orazem, Nadine Pébère, Bernard Tribollet, Vincent Vivier

Determination of water uptake in organic coatings deposited on 2024 aluminium alloy: comparison between impedance measurements and gravimetry

Anh Son Nguyen[a,b], Nicolas Caussé[a], Marco Musiani[c], Mark E. Orazem[d], Nadine Pébère[a,*], Bernard Tribollet[e], Vincent Vivier[e]

[a] *CIRIMAT, Université de Toulouse, CNRS, INPT, UPS, ENSIACET, 4, allée Emile Monso, BP 44362, 31030 Toulouse cedex 4, France*

[b] *Laboratory for Protective Coatings, Institute for Tropical Technology, VAST, 18, Hoang Quoc Viet, Hanoi, Vietnam*

[c] *Institute of Condensed Matter Chemistry and Technologies for Energy, ICMATE - CNR, Corso Stati Uniti 4, 35127 Padova, Italy*

[d] *Department of Chemical Engineering, University of Florida, Gainesville, Florida 32611, USA*

[e] *Sorbonne Universités, UPMC Université Paris 06, CNRS, Laboratoire Interfaces et Systèmes Electrochimiques, 4 place Jussieu, F-75005, Paris, France*

* Corresponding author.
Phone: 00 33 5 34 32 34 23
Fax: 00 33 5 34 32 34 99
E-mail: Nadine.Pebere@ensiacet.fr (Nadine Pébère)

Abstract

Electrochemical impedance spectroscopy (EIS) and gravimetric measurements on two water-based coatings, containing either $SrCrO_4$ or a mixture of Cr(VI)-free pigments and deposited on 2024 aluminium alloy, were performed to follow the water uptake in a 0.5 M NaCl solution as a function of exposure time. To account for the observed non-ideal capacitive behaviour, the coating capacitance and dielectric constant values were extracted from the EIS data in two ways: (i) by using a complex-capacitance representation and (ii) by fitting to the EIS data a model that assumed an exponential distribution of coating resistivity. The agreement of values obtained by these independent methods served to validate the model used to account for the observed pseudo constant-phase-element (CPE) behaviour of the coatings. The water uptake calculated from dielectric constant values, employing a linear combination formula, was in good agreement with that directly measured by gravimetry, using supported-films.

Keywords: water-based protective coatings, electrochemical impedance, complex-capacitance, resistivity distribution, water uptake

1. Introduction

In a series of recent papers [1-5], our group has studied laboratory and industrial coatings by electrochemical impedance spectroscopy (EIS), with the objective of finding physically sound models to account for their non-ideal capacitive behaviour. Models assuming distribution of coating resistivity and uniform dielectric constants provided good account for the experimental data. Constant-phase-element (CPE) behaviour was observed for aluminium alloy/hybrid sol-gel coating samples immersed in NaCl solutions and was attributed to local resistivity distributions following a power law [1, 2]. We have previously shown that a power-law resistivity profile caused CPE behaviour [6-8]; whereas, an exponential resistivity profile, discussed by Young [9-10] and by Schiller and Strunz [11], caused a continuous, though mild, variation of phase angle with frequency. The need to consider position-dependent properties of the coating materials had been previously pointed out by other authors [12-14] who, however, did not propose specific resistivity-position dependencies. Based on the observation that coatings that behaved as quasi-ideal when they were dry became increasingly non-ideal upon immersion in electrolytes [3], we attributed the formation of resistivity profiles to inhomogeneous penetration of water and ions into the coatings. Models for the behaviour of industrial coatings, which did not correspond to a CPE, required considering exponential resistivity-position profiles extending over either the entire coating thickness or just part of it [3, 4]. As power-law and exponential dependencies are only two mathematically simple cases of more general resistivity-position relationships, we have proposed the use of Voigt measurement model [15] for the identification of resistivity distributions that cause frequency dispersion in the EIS response of coatings [5].

The importance of assessing the water uptake into coatings has been acknowledged for some decades because water penetration is an initial step in the degradation process. The knowledge

of the resistivity profile is insufficient to determine the water uptake in the coatings [2] because the ion concentration in the water that penetrates the film is normally unknown and probably much different from the concentration in the test electrolyte [16, 17]. In principle, water uptake can be estimated from resistance data when EIS tests are performed with coatings exposed to pure water [18, 19], although, even in this case, the resistivity of the electrolyte within the coating can be affected by ionic species initially present in the coating that become dissolved in water. Since our previous work [1-5] focused on assessing resistivity profiles, we did not discuss water uptake, and actually used the "water volume fraction" only as a formal intermediate parameter in calculations, without a direct physical meaning. In the present paper, we discuss water uptake in industrial coatings containing either strontium chromate or environmentally friendly inhibitors [4], focusing on the evolution of coating capacitance during prolonged exposure, and comparing the EIS-derived values with gravimetric measurements.

The determination of coating dielectric constant, the calculation of water uptake therefrom, and the comparison with direct gravimetric measurements have been the object of many studies. Reports in the literature include studies in which both EIS and gravimetric measurements were made on metal-supported coatings [12, 16-22], where both were made on free-standing films [12, 23-26], and where impedance was measured with supported coatings and mass variation with free films [27-29]. Different authors have put forward reasons for preferring free films or supported coatings. Gravimetric measurements may be more reliable when performed with free films because, in supported coatings, corrosion reactions occurring at the metal/coating interface may induce mass changes [12]. However, when corrosion is negligible, i.e., for highly adhesive and protective coatings and moderate durations of the exposure to electrolytic solutions, metal-supported coatings are more representative of practical application as compared to free films. In particular, some properties can differ due to changes in chemistry

resulting from specific interactions with metal substrates, such as aluminium, during curing reaction [30, 31].

Two critical aspects of the EIS/gravimetry comparison are: (i) the determination of the coating capacitance, from which dielectric constant is computed, given the sample geometry, and (ii) the calculation of water uptake from dielectric constant data. The former aspect requires special care when the coatings do not behave as ideal capacitors, and, thus, the capacitance must be computed from CPE parameters [8, 32]. Although other effective medium formulas have been proposed [33], the most popular formula for the conversion of dielectric constant to water volume fraction, henceforth called the BK formula, was proposed by Brasher and Kingsbury [34]. Different authors who compared water uptake values calculated following the BK formula to gravimetric measurements reached diverging conclusions on its reliability. For example, Lindquist [20] took into account various alternative equations, finding that the BK formula gave the best results; Castela and Simões [21] found that values calculated with the BK formula were far from gravimetric values and a calculation based on a linear combination of dielectric constants provided better agreement; Sauvant-Moynot et al. [26] reported that the BK equation yielded water uptake values either in good agreement with gravimetry or not, depending on the investigated system, as was already indicated by Brasher and Kingsbury [34]. Various authors [20-23, 26, 27] observed a tendency of the BK formula to overestimate water uptake. A modified formula proposed by Sykes [35], who removed a possibly unjustified approximation from Brasher and Kingsbury calculation, leads to even stronger overestimations. Vosgien Lacombe et al. [36] have recently shown that the BK formula yields water uptake values in agreement with gravimetry if coating swelling is taken into account. These authors have suggested that unjustified assumption of negligible swelling probably explains reported water uptake values calculated according to the BK formula that were larger or much larger than those determined by gravimetry.

In the present work, we report on new experiments aimed at measuring the water uptake for the same coatings studied in [4] and on a deeper analysis of the EIS data reported therein. The coating capacitance and dielectric constant were determined in two independent ways: (i) the coating dielectric constant was an adjustable parameter in the fitting of EIS data using a model that assumed an exponential distribution of coating resistivity as previously described in [4], or (ii) the coating capacitance was determined from complex- capacitance plots (Cole-Cole plots) and the dielectric constant was calculated following the equation for the capacity of a plane capacitor. Then, we used the BK formula, its Sykes variant and a linear equations for the dielectric constant-water uptake conversion. Comparison of water uptake calculated from EIS and gravimetric data provided a further test of the validity of the model [4].

2. Experimental

2.1. Coating samples

Two water-based paints were deposited by air spraying onto 2024 T3 aluminium alloy currently used in the aerospace industry. The chemical composition in weight percent of the alloy was: Cu: 4.90; Mg: 1.31; Mn: 0.56; Si: 0.08; Fe: 0.26; Zn: 0.10; Ti: 0.01 and Al to balance. The specimens consisted of 125 mm × 80 mm × 1.6 mm plates machined from a rolled plate. Before painting, the samples were degreased at 60°C (pH = 9) for 15 min, rinsed twice with distilled water, then etched in an acid bath at 52 °C for 10 min, and rinsed again with distilled water. The liquid paints were applied by air spraying and cured at 60°C. Both paints, manufactured by Mapaero SAS, Pamiers, France, had the same polymer matrix (based on a bisphenol A epoxy polymer and a polyaminoamide) and contained the same fillers, i.e. 12 wt. % TiO_2, 11 wt. % talc and 1 wt. % SiO_2, but different inhibitors. One of them (henceforth called CC) contained 16 wt. % of $SrCrO_4$, the other was a Cr(VI)-free coating (called NCC) which

contained 10 wt. % of a mixture of ZnO and a phosphosilicate. The ratio of the pigment volume concentration (PVC) to critical pigment volume concentration (CPVC) was optimized for both coatings (about 0.6). The coatings were 21 ± 2 μm and 18 ± 2 μm thick for CC and NCC, respectively.

2.2. Gravimetric experiments and chromate leaching

The water uptake was measured at room temperature (20 ± 2°C) on metal-supported coatings. To minimize the mass difference between the aluminium plate and the coating, the CC and NCC water-based films were applied on 50 μm-thick aluminium foils, (purity 99.0 %) (Goodfellow), without any surface preparation, and cured at 60°C. Square samples (3 cm x 3 cm) were cut from the coated foils. Before immersion in 100 mL of 0.5 M NaCl solution, each sample was weighed on a Mettler balance with a precision of 0.1 mg. Samples were periodically removed from the NaCl solution and weighed, after carefully removing the water excess from coatings surface with filter paper. At the end of the exposure, the films were peeled piece by piece from the aluminium foil and the foil was weighed.

The sample mass before immersion, after immersion and after coating removal are denoted m_1, m_2 and m_0, respectively. Each value was obtained by averaging at least 5 measurements.

The leaching of $SrCrO_4$ from CC was measured with the procedure described in [4] and summarized briefly here. A cylindrical Plexiglas tube was fixed on top of the CC sample and filled with 100 mL of a 0.5 M NaCl solution. A 5 mL aliquot of the solution was periodically removed and replaced with 5 mL of fresh 0.5 M NaCl solution to maintain a constant volume at 100 mL. The concentrations of released chromate ions were determined by UV-visible spectroscopy using a Shimadzu UV 1800 at λ = 371 nm. A calibration curve was built by analysing standard strontium chromate solutions. Dilution effects were taken into account. The

leaching experiments showed that $SrCrO_4$ was progressively lost by CC samples during exposure to the NaCl solution. Its mass, function of immersion duration, is denoted m_{SrCrO4}. No comparable phenomena were observed with NCC.

The mass fraction of water (ϕ_m) absorbed by the coating for each exposure time was calculated as

$$\phi_m = \frac{m_2 - m_1 + m_{SrCrO4}}{m_2 - m_0} \quad (1)$$

with $m_{SrCrO4} = 0$ for NCC, and the appropriate m_{SrCrO4} value at each immersion time for CC. In the following sections, water uptake is expressed as percent mass variation, rather than mass fraction, as it is usually done by most authors.

Since the formulas used to compute water uptake from dielectric constants [33-35] are written in terms of volume fractions (ϕ) this quantity was calculated as

$$\phi = \frac{d_c}{\frac{1}{\phi_m} - 1 + d_c} \quad (2)$$

where d_c is the density of the coatings, assumed identical for both CC and NCC, and equal to 1.7 g cm^{-3}.

2.3. Electrochemical impedance measurements

Impedance measurements were carried out in a three-electrode cell, in which the coated specimen served as the working electrode. A saturated calomel electrode and a large platinum sheet were used as reference and counter electrode, respectively. All tests were performed in 0.5 M NaCl solution, at the open circuit potential. The working electrode surface area was 24 cm^2. The electrochemical cell was open to air and was kept at room temperature (20 °C ± 2 °C). Electrochemical impedance measurements were carried out using a Biologic VSP apparatus. The impedance diagrams were obtained, for exposure times ranging from 2 to 504 h, under

potentiostatic conditions, at the corrosion potential, over a frequency range of 65 kHz to 1 Hz with 8 points per decade, using a 30 mV peak-to-peak sinusoidal voltage perturbation. The results shown for a single coating were typical of other nominally identical coatings, but statistical analysis was not performed.

The best fitted values of the model parameters were determined with a non-commercial software developed at the LISE CNRS, Paris, which allows the use of combinations of passive circuit elements and analytic expressions.

3. Results and discussion

It has been shown by Jonscher that the capacitance of a dielectric layer can be determined by extrapolation of the complex-capacitance plots to infinite frequency, using the complex-capacitance representation [37, 38]. This approach does not require assumption of any specific model. Dielectric constants can also be determined by fitting EIS data. In our previous work [4], a model that assumed an exponential distribution of coating resistivity was proposed, but the dielectric constants, assumed to be uniform throughout the coatings, and their evolution with immersion time were not discussed and validated by comparison with values determined with an independent method of EIS data analysis. Therefore, a first aim of the present work has been to check the consistency of dielectric constant data obtained from complex-capacitance plots and model fitting.

The complex-capacitance plots may be obtained from impedance data by using the transformation

$$C(\omega) = \frac{1}{\mathrm{j}\omega[Z(\omega) - R_e]} \qquad (3)$$

which requires an estimation of the electrolyte resistance R_e and its subtraction from the real part of the impedance. Once the coating capacitance is known, the coating dielectric constant

(ε_w) is computed from the usual relationship expressing the capacitance of a plane capacitor, *i.e.,*

$$\varepsilon_w = \frac{C_c \delta}{\varepsilon_0} \tag{4}$$

where ε_w, ε_0 and δ represent, respectively, the dielectric constant of the coating under "wet conditions", the vacuum permittivity, and the thickness of the coating.

In the following sections, we examine the effect of an inaccurate determination/correction of R_e, using synthetic impedance data calculated for an exponential distribution of resistivity, i.e. for the so-called Young impedance. Then, we describe the use of complex-capacitance plots to extract the coating capacitance (C_c) of CC and NCC coatings, as a function of exposure time to the NaCl solution.

3.1. Complex-capacitance plots of synthetic impedance data

Synthetic impedance data calculated for an exponential distribution of the coating resistivity were considered because this resistivity profile allowed the impedance data of CC and NCC samples to be reproduced with good accuracy [4].

The exponential distribution of resistivity may be written

$$\rho(x) = \rho_0 \exp(-\frac{x}{\lambda}) \tag{5}$$

and the corresponding Young impedance is given by

$$Z = -\frac{\lambda}{j\omega\varepsilon_w\varepsilon_0} \ln\left(\frac{1 + j\omega\varepsilon_w\varepsilon_0\rho_0 e^{-\delta/\lambda}}{1 + j\omega\varepsilon_w\varepsilon_0\rho_0}\right) \tag{6}$$

In both equations (5) and (6), ρ_0 represents the coating resistivity at the metal/coating interface. The parameter λ indicates how sharply the resistivity changes with position (a larger λ corresponds to a smoother resistivity profile). Fig. 1 shows the synthetic Young impedance data generated following Eq. (6), using values of ε_w, ρ_0 and δ close to those measured for the CC

and NCC samples [4] and an R_e value fixed at 300 Ω cm^2 (non-corrected curve in Fig. 1). The upper frequency limit used in calculating the data shown in Fig. 1 was 10 MHz, much larger than that attainable with most electrochemical equipment, which is typically of the order of 100 kHz. The use of reference electrodes may further decrease this upper limit. Thus, an accurate determination of R_e from the impedance data in Fig. 1, and in many experimental cases, is impossible in the accessible frequency range (see, in particular Fig. 1b').

In addition to the non-corrected curve, Fig. 1 shows ohmic-resistance corrected Bode diagrams [39] obtained for various values of R_e, including the correct value (300 Ω cm^2), overestimated values (330 and 600 Ω cm^2) and underestimated values (150 and 270 Ω cm^2). Phase angle plots (especially the expanded Fig. 1b') show that, only when the data are corrected using the accurate value, R_e = 300 Ω cm^2, the curve becomes tangent to the θ = -90° line. Overcorrection yields curves that cross the θ = -90° line; whereas, correction with underestimated R_e values yields curves that never attain θ = -90°.

Fig. 2a presents the complex-capacitance plots corresponding to the curves presented in Fig. 1, obtained by using Eq. (3). Only the high-frequency range used to extract the capacitance values is shown in Fig. 2. Table 1 summarizes the dielectric constant values calculated according to Eq. (4) from the coating capacitance values obtained for $C_j = 0$ for different R_e values, and the errors on the dielectric constant made by overestimating R_e. For underestimated R_e values, the complex-capacitance plots did not cross the C_r axis and no capacity values were determined (n.d., in Table 1). The error values show that, if R_e is determined with a +10 % precision, the error on dielectric constant is 0.4 %. Even if R_e is 100 % overestimated, the error on dielectric constant is small (3.1 %). These conclusions on the accuracy of the determination of dielectric constant are specific to the set of parameters employed in the calculation of synthetic impedance, which were appropriate for coatings. However, similar analysis with

synthetic data with parameters corresponding to oxide films, for example 10 nm thick, showed that the error on the determination of the capacitance could be much higher (not shown here). It is interesting to see that, with the accurate correction of the electrolyte resistance, the capacitance value can be directly read at high frequency on the *x* axis, but not in the measurable frequency range, and is 4.425 x 10^{-10} F cm^{-2}.

As will be presented in the next section with the experimental data, the upper frequency measured was 65 kHz. Thus, for the synthetic data, the coating capacitance values were determined by using this last frequency point in the complex-capacitance plots and by extrapolation with a vertical line crossing the C_r axis (Fig. 2b). The capacitance values are reported in Table 2 and the errors made on dielectric constant were calculated by comparison with the true value (ε = 10). The errors calculated by this approximation to determine the dielectric constant is small (2.6 % to 3.4 %) and, thus, this methodology will be used to extract the capacitance on the experimental data in the next section.

3.2. Complex-capacitance plots of experimental impedance data

Fig. 3 shows the Bode plots for the CC and NCC coatings after 10, 24, and 168 h immersion in 0.5 M NaCl solution. Comparable impedance plots were already published and analysed in [4]. The solid lines in Fig. 3 are the best-fitted curves obtained by regressing Eq. (7) to the data.

$$Z = d\frac{\rho_c}{(1+j\omega\varepsilon_c\varepsilon_0\rho_c)} + \left\{\frac{1}{R_{pore}} - \left[\frac{\lambda}{j\omega\varepsilon_w\varepsilon_0}\ln\left(\frac{1+j\omega\varepsilon_w\varepsilon_0\rho_c e^{-(\delta-d)/\lambda}}{1+j\omega\varepsilon_w\varepsilon_0\rho_c}\right)\right]^{-1}\right\}^{-1} + R_e \qquad (7)$$

Equation (7) expresses the series combination of three impedances corresponding to: an inner layer of thickness *d* with purely capacitive behaviour, an outer layer of thickness (δ - *d*) whose impedance is given by a Young impedance in parallel with a pore resistance (R_{pore}), and the electrolyte. The first term of the right hand side (inner layer) is proportional to *d* and therefore vanishes when the resistivity becomes position dependent across the whole coating

thickness [4]. Once d becomes equal to zero, the impedance of the entire coating is given by the second term in Eq. (7). This equation allows the determination of R_e, λ, ε_w, R_{pore} and d as adjustable parameters. The lines in Fig. 3 represent the fitted curves calculated according to Eq. (7), and prove the good agreement between experimental points and model.

Fig. 4 shows the complex-capacitance plots corresponding to EIS spectra of CC and NCC, obtained after 10 h, 1 week, and 1 month immersion in 0.5 M NaCl solution. The R_e values used for the conversion from impedance to complex capacitance were those determined through the regression of Eq. (7). The R_e values were 246 ± 21 Ω cm^2 for the NCC sample and 364 ± 69 Ω cm^2 for the CC sample. Capacitances were determined by extrapolation of the high-frequency $C(\omega)$ data to the real axis (vertical line crossing the C_r axis ($C_j = 0$) as shown in Fig. 4).

Fig. 5 compares the time-dependence of the capacitances of CC and NCC obtained from the complex-capacitance plots. For both coatings, the capacitance increases faster during the first 24-48 h of immersion (visible in linear scale for the immersion time). Then, after 168 h of immersion, the CC and NCC capacitances keep increasing and the curves are almost parallel. The difference between the capacitance values for the two systems could be attributed both to a difference in microstructure, linked to the presence of different inhibitive pigments, and to the coating thickness.

The dielectric constant values (ε_w), were calculated from the capacitance values, using Eq. (4) with δ = 21 μm and 18 μm for CC and NCC, respectively. The ε_w values are shown in Fig. 6, as a function of exposure time, together with the values obtained from regression of Eq. (7), using all data points in the frequency range 65 kHz - 1 Hz. The dielectric constants of the dry coatings [4] are also indicated. For the NCC sample, the dielectric constant values obtained by both methods are nearly the same. For the CC sample, during the first 24 h, the ε_w values are similar, but diverge for longer immersion times (> 168 h). The uncertainty in the dielectric

constant obtained from complex-capacitance plots is smaller than the deviation observed at long times between the value obtained by regression of the Young model and the value obtained from the complex-capacitance plots. The observed discrepancy could be explained by the leaching of chromates that resulted in a non-exponential resistivity profile [4] and to the fact that the two methods take into account different frequency ranges, wider for regression of Eq. (7), narrower and restricted to high frequency for the complex-capacitance analysis.

The global agreement between the two methods is quite good, which contributes to validate the model proposed in [4]. Although CC and NCC had the same polymer matrix and contained the same fillers, their ε_w-time curves obtained from the complex-capacitance plots were not totally similar (Fig. 6). This result, in agreement with those of other workers [40], confirmed that the nature and morphology of the inhibitive pigments within the coatings induced differences in their microstructure. The higher dielectric constant values obtained for the CC sample after one month of immersion (from the complex-capacitance plots) would be indicative of a higher water uptake likely due to the chromates leaching which induces a modification of the microstructure of the coating [4].

3.3. Gravimetric measurements

Fig. 7a shows the mass variation of CC and NCC samples during immersion in 0.5 M NaCl solution. The mass variation of the CC sample was corrected by taking into account, through Eq. (1), the release of $SrCrO_4$ into the test solution, demonstrated by the plot in Fig. 7b. The $SrCrO_4$ released at the end of the experiment was 5.6 wt. % of its initial value, *i.e.* 1.13 wt. % of the coating weight. A comparable correction was not necessary for the NCC. The leaching of the inhibitive species could be neglected for the NCC because it was shown [4] that the impedance diagrams of NCC measured in dry condition before immersion and after ageing were similar. This was not the case for the CC sample. The impedance of dry CC underwent

significant and irreversible modifications after immersion in NaCl solution and successive aging due to the dissolution of $SrCrO_4$.

3.4. Comparison of the water uptake determined by the different methodologies

The relationships most commonly used to calculate the water uptake from impedance data are:

- A linear relationship:

$$\varepsilon_w = \varepsilon_c (1 - \phi) + \varepsilon_{water} \phi \quad (8)$$

- The Brasher and Kingsbury formula [34]:

$$\log(\varepsilon_w) = \log(\varepsilon_c) + \log(\varepsilon_{water}) \phi \quad (9)$$

- The Sykes formula [35] (a variant of the Brasher and Kingsbury formula):

$$\log(\varepsilon_w) = \log(\varepsilon_c) (1 - \phi) + \log(\varepsilon_{water}) \phi \quad (10)$$

In equations (8)-(10), ε_w, ε_c and ε_{water} are the dielectric constants of the coating after immersion in the electrolyte (determined from the capacitance in the complex-capacitance plots (Fig. 4)), of the dry coating and of the water, respectively, and ϕ is the volume fraction of water in the coating. The parameters ε_w, and ϕ vary with the duration of immersion.

Fig. 8 compares the water uptake determined with the gravimetric method and from equations (8), (9) and (10). Using Eq. (8), linear combination, an almost perfect agreement was observed for CC; whereas, for NCC the water uptake measured by gravimetry was systematically lower by ca 1.5 m% than that obtained from the impedance data. The Brasher and Kingsbury formula, Eq. (9) and the Sykes formula, Eq. (10), yielded water uptake values much higher than those measured directly by gravimetry (for example, for NCC, 11 m% and 20 m%, respectively, at 336 h immersion), as previously reported in the literature [20-23, 26, 27]. Possible causes of the imperfect agreement obtained for NCC include an inaccurate value of the coating thickness, the loss of some water during the operations between emersion of the

sample from the test solution and its weighing and, of course, the fact that Eq. (8), as well as other formulas, may be more or less adequate for different systems.

The water uptake after 336 h of immersion in the NaCl solution measured by gravimetry was slightly higher for the CC (5 m%) than for the NCC (4 m%), probably due to water filling the voids left by $SrCrO_4$ leaching. If referred only to the polymer matrix mass (60% and 66% of the total mass for CC and NCC, respectively) the water uptake was 8.3 m% for CC and ca. 6.1 m% for NCC.

The swelling of the coating was not considered in the present work. Even the highest swelling values reported by other authors [36] would not cause an error higher than 5% in the determination of the dielectric constant. Under the assumption of a linear propagation of errors following Eq. (8), such a change in the value of the dielectric constant would increase the water uptake by 0.5 m%. This increase is in the order of the size of the symbols used in Fig. 8.

4. Conclusions

Water uptake has been studied in $SrCrO_4$-containing (CC) and Cr(VI)-free (NCC) coatings immersed in 0.5 M NaCl solutions using EIS and gravimetry. Complex-capacitance plots were shown to be useful for assessing the capacitance, and hence the dielectric constant, of coatings exposed to an electrolyte, even when an accurate determination of the electrolyte resistance, necessary for the impedance/capacitance conversion, is prevented due to an insufficiently wide frequency range accessible in EIS measurements. The dielectric constant values derived from complex-capacitance analysis were in good agreement with those determined by regression of the EIS data using a model that assumed an exponential distribution of coating resistivity, previously described in [4], and contributed to validate the model. For these coatings, the water uptake values calculated from dielectric constant values were in good agreement with those

obtained by direct gravimetric measurements, provided a linear combination of polymer and water dielectric constants were used. The agreement was almost perfect for $SrCrO_4$-containing coatings and slightly less satisfactory for coatings containing Cr(VI)-free inhibitive pigments. In contrast, the Brasher and Kingsbury formula [34] and its variant, the Sykes formula [35], yielded water uptake values that greatly exceeded the gravimetric ones (up to five times larger for long immersion times). This conclusion, in agreement with those of other workers, is specific to our systems. We do not claim it to be of general validity. Finally, the larger water uptake in $SrCrO_4$-containing coatings than in Cr(VI)-free ones was probably due to the fact that, in addition to ordinary uptake, water filled the voids left by $SrCrO_4$ leaching.

Acknowledgments

The authors gratefully acknowledge the company MAPAERO (Pamiers, France) for the preparation of the coated samples and more particularly Pauline Côte and Pierre-Jean Lathière for fruitful discussion on coating technologies. Mark E. Orazem expresses appreciation for the support of this collaboration from the ExxonMobil Gator Chemical Engineering Alumni Term Professorship. The PhD thesis of Nguyen Anh Son was prepared in the framework of the associated international laboratory "Functional Composite Materials (FOCOMAT)" between France and Vietnam.

References

[1] S. Amand, M. Musiani, M. Orazem, N. Pébère, B. Tribollet, V. Vivier, Constant-Phase-Element Behavior Caused by Inhomogeneous Water Uptake in Anti-Corrosion Coatings, Electrochim. Acta 87 (2013) 693-700.

[2] M. Musiani, M. Orazem, N. Pébère, B. Tribollet, V. Vivier, Determination of Resistivity Profiles in Anti-Corrosion Coatings from Constant-Phase-Element Parameters, Prog. Org. Coat. 77 (2014) 2076-2083.

[3] A.S. Nguyen, M. Musiani, M.E. Orazem, Nadine Pébère, B. Tribollet, V. Vivier, EIS analysis of the distributed resistivity of coatings in dry and wet conditions, Electrochim. Acta. 179 (2015) 452-459.

[4] A.S. Nguyen, M. Musiani, M.E. Orazem, N. Pébère, B. Tribollet, V. Vivier, Impedance study of the influence of chromates on the properties of waterborne coatings deposited on 2024 aluminium alloy, Corros. Sci. 109 (2016) 174-181.

[5] Y.-M. Chen, A.S. Nguyen, M.E. Orazem, B. Tribollet, N. Pébère, M. Musiani, V. Vivier, Identification of Resistivity Distributions in Dielectric Layers by Measurement Model Analysis of Impedance Spectroscopy, Electrochim. Acta 219 (2016) 312-320.

[6] B. Hirschorn, M. E. Orazem, B. Tribollet, V. Vivier, I. Frateur, M. Musiani, Constant-Phase-Element Behavior Caused by Resistivity Distributions in Films: 1. Theory, J. Electrochem. Soc. 157 (2010) C452-C457.

[7] B. Hirschorn, M. E. Orazem, B. Tribollet, V. Vivier, I. Frateur, M. Musiani, Constant-Phase-Element Behavior Caused by Resistivity Distributions in Films: 2. Applications, J. Electrochem. Soc. 157 (2010) C458-C463.

[8] M.E. Orazem, I. Frateur, B. Tribollet, V. Vivier, S. Marcelin, N. Pébère, A.L. Bunge, E.A. White, D.P. Riemer, M. Musiani, Dielectric Properties of Materials showing Constant-Phase-Element (CPE) Impedance Response, J. Electrochem. Soc. 160 (2013) C215-C225.

[9] L. Young, Anodic oxide films 4: The interpretation of impedance measurements on oxide coated electrodes on niobium, Transactions of the Faraday Society 51(1955) 1250-1260.

[10] L. Young, Anodic Oxide Films, Academic Press, New York, 1961.

[11] C.A. Schiller, W. Strunz, The evaluation of experimental dielectric data of barrier coatings by means of different models, Electrochim. Acta, 46 (2001) 3619-3625.

[12] F. Bellucci, L. Nicodemo, Water transport in organic coatings, Corrosion NACE 49 (1993) 235-247.

[13] J. Kittel, N. Celati, M. Keddam, H. Takenouti, New methods for the study of organic coatings by EIS: new insights into attached and free films, Prog. Org. Coat. 41 (2001) 93-98.
[14] J. Kittel, N. Celati, M. Keddam, H. Takenouti, Influence of the coating-substrate interactions on the corrosion protection: Characterisation by impedance spectroscopy of the inner and outer parts of a coating, Prog. Org. Coat. 46 (2003) 135-147.
[15] P. Agarwal, M.E. Orazem, L.H. García-Rubio, Measurement models for electrochemical impedance spectroscopy: 1. Demonstration of applicability, J. Electrochem. Soc. 139 (1992) 1917-1927.
[16] V.B. Mišković-Stanković, D.M. Dražić, M.J. Teodorović, Electrolyte penetration through epoxy coatings electrodeposited on steel, Corros. Sci. 37 (1995) 241-252.
[17] V.B. Mišković-Stanković, D.M. Dražić, Z. Kačarević-Popović, The sorption characteristics of epoxy coatings electrodeposited on steel during exposure to different corrosive agents, Corros. Sci. 38 (1996) 1513-1523.
[18] E.P.M. Van Westing, G.M. Ferrari, J.H.W. De Wit, The determination of coating performance with impedance measurements - II. Water uptake of coatings, Corros. Sci. 36 (1994) 957-977.
[19] A. Cao-Paz, A. Covelo, J. Fariña, X.R. Nóvoa, C. Pérez, L. Rodríguez-Pardo, Ingress of water into organic coatings: Real-time monitoring of the capacitance and increase in mass, Prog. Org. Coat. 69 (2010) 150–157.
[20] S.A. Lindquist, Theory of dielectric properties of heterogeneous substances applied to water in a paint film, Corrosion NACE 41 (1985) 69-75.
[21] A.S. Castela, A.M. Simões, Assessment of water uptake in coil coatings by capacitance measurements, Prog. Org. Coat. 46 (2003) 55-61.
[22] L.V.S. Philippe, S.B. Lyon, C. Sammon, J. Yarwood, Validation of electrochemical impedance measurements for water sorption into epoxy coatings using gravimetry and infra-red spectroscopy, Corros. Sci., 50 (2008) 887-896.
[23] A.S. Castela, A.M. Simões, An impedance model for the estimation of water absorption in organic coatings. Part I: A linear dielectric mixture equation, Corros. Sci. 45 (2003) 1631-1646.
[24] A.S. Castela, A.M. Simões, Water sorption in freestanding PVC films by capacitance measurements, Prog. Org. Coat. 46 (2003) 130-134.
[25] R.G. Duarte, A.S. Castela, M.G.S. Ferreira, Influence of the solution cation mobility on the water uptake estimation of PVC Plastisol freestanding films by EIS, Prog. Org. Coat. 57 (2006) 408-415.

[26] V. Sauvant-Moynot, S. Duval, N. Gimenez, J. Kittel, Hot wet aging of glass syntactic foam coatings monitored by impedance spectroscopy, Prog. Org. Coat. 59 (2007) 179-185.
[27] V.N. Nguyen, F.X. Perrin, J.L. Vernet, Water permeability of organic/inorganic hybrid coatings prepared by sol-gel method: a comparison between gravimetric and capacitance measurements and evaluation of non-Fickian sorption models, Corros. Sci. 47 (2005) 397-412.
[28] G. Lendvay-Győrik, T. Pajkossy, B. Lengyel, Corrosion-protection properties of water-borne paint coatings as studied by electrochemical impedance spectroscopy and gravimetry, Prog. Org. Coat. 56 (2006) 304-310.
[29] N. Fredj, S. Cohendoz, S. Mallarino, X. Feaugas, S. Touzain, Evidencing antagonist effects of water uptake and leaching processes in marine organic coatings by gravimetry and EIS, Prog. Org. Coat. 67 (2010) 287-295.
[30] A.A. Roche, J. Bouchet, S. Bentadjine, Formation of epoxy-diamine/metal interphases, Int. J. Adhes. Adhes. 22 (2002) 431-41.
[31] N. Causse, L. Quiroga Cortes, E. Dantras, C. Tonon, M. Chevalier, H. Combes, P. Guigue, C. Lacabanne, New bonded assembly configuration for dynamic mechanical analysis of adhesives, Int. J. Adhes. Adhes. 46 (2013) 1-6.
[32] B. Hirschorn, M.E. Orazem, B. Tribollet, V. Vivier, I. Frateur, M. Musiani, Determination of Effective Capacitance and Film Thickness from CPE Parameters, Electrochim. Acta 55 (2010) 6218-6227.
[33] B. Hinderliter, S. Croll, D. Tallman, Q. Su, G. Bierwagen, Interpretation of EIS data from accelerated exposure of coated metals based on modeling of coating physical properties, Electrochim. Acta 51 (2006) 4505-4515.
[34] D.M. Brasher, A.H. Kingsbury, Electrical measurements in the study of immersed paint coatings on metal. I. Comparison between capacitance and gravimetric methods of estimating water-uptake. J. Appl. Chem. 4 (1954) 62-72.
[35] J.M. Sykes, A variant of the Brasher-Kingsbury equation, Corros. Sci. 46 (2004) 515-517.
[36] C. Vosgien Lacombe, G. Bouvet, D. Trinh, S. Mallarino, S. Touzain, Water uptake in free films and coatings using the Brasher and Kingsbury equation: a possible explanation of the different values obtained by electrochemical impedance spectroscopy and gravimetry, Electrochim. Acta 231 (2017) 162-170.
[37] A.K. Jonscher, Admittance spectroscopy of systems showing low-frequency dispersion, Electrochim. Acta 35 (1990) 1595-1600.
[38] A.K. Jonscher, Dielectric characterization of semiconductors, Solid-State Electronics, 33 (1990) 737-742.

[39] M.E. Orazem, N. Pébère, B. Tribollet, Enhanced graphical representation of electrochemical impedance data, J. Electrochem. Soc., 153 (2006) B129.
[40] L. Fedrizzi, F. Deflorian, G. Boni, P.L. Bonora, E. Pasini, EIS study of environmentally friendly coil coating performances, Prog. Org. Coat. 29 (1996) 89-96.

Table 1: Capacitance values obtained from the complex-capacitance plots at $C_j = 0$ (Fig. 2a) and dielectric constant values calculated according to Eq. (4) for different R_e values.

R_e (Ω cm^2)	Capacitance (F cm^{-2})	Dielectric constant	Error (%)
150 (-50 %)	n.d.	-	-
270 (-10 %)	n.d.	-	-
300 (0 %)	4.425×10^{-10}	10.00	0
330 (10 %)	4.442×10^{-10}	10.04	0.4
600 (100 %)	4.562×10^{-10}	10.31	3.1

Table 2: Capacitance values obtained from the complex-capacitance plots from a vertical line at 65 kHz crossing the C_r axis (Fig. 2b) and dielectric constant values calculated according to Eq. (4) for different R_e values. The errors account for the difference between the true dielectric constant ($\varepsilon = 10$) and the determined value

R_e (Ω cm^2)	Capacitance (F cm^{-2})	Dielectric constant	Error (%)
150	4.539×10^{-10}	10.26	2.6
270	4.555×10^{-10}	10.29	2.9
300	4.559×10^{-10}	10.30	3.0
330	4.562×10^{-10}	10.31	3.1
600	4.576×10^{-10}	10.34	3.4

Figure captions

Fig. 1: Synthetic impedance calculated for a Young impedance, Eq. (6), in series with an electrolyte resistance, with: δ = 20 µm, $\rho_0 = 10^{13}$ Ω cm, $\lambda = 1.3\ 10^{-4}$ cm, $\varepsilon_w = 10$, $R_e = 300$ Ω cm^2. The uncorrected curves and curves corrected with different R_e values indicated on the figure are shown. Parts (a') and (b') are expanded views of parts (a) and (b), relevant to the high frequency region.

Fig. 2: Influence of the R_e value used for the conversion of the calculated impedance shown in Fig. 1 to capacitance. Complex-capacitance plots are shown for the R_e values indicated on the figure. (a) high frequency region and (b) same curves truncated at 65 kHz (measured frequency limit in this work).

Fig. 3: Impedance responses in Bode format for the AA2024 coated samples (CC and NCC) after 10 h, 24 h and 168 h of immersion in 0.5 M NaCl solution. The solid lines are the best fitted curves according to Eq. (7).

Fig. 4: Complex-capacitance plots corresponding to EIS spectra of CC and NCC obtained after 10 h, 1 week and 1 month of immersion in 0.5 M NaCl solution. The axis are not orthonormal to make the extrapolation to the C_r axis better visible.

Fig. 5: Variation of the capacitance obtained from the complex-capacitance plots (at 65 kHz) for CC and NCC as a function of immersion time in 0.5 M NaCl).

Fig. 6: Comparison of the wet dielectric constant (ε_w) obtained from the impedance data analysis (in the frequency range 65 kHz to 1 Hz) and from the complex-capacitance plots at 65 kHz.

Fig. 7: (a) Percent mass variation (m %) vs. immersion time in 0.5 M NaCl for CC and NCC (supported coatings on a thin Al foil) obtained from gravimetric method at room temperature. Error bars account from at least five independent measurements. (b) Immersion time dependence of the amount of $SrCrO_4$ released from a CC sample in contact with a 0.5 M NaCl solution.

Fig. 8: Comparison of the water uptake (m %) for (a) CC and (b) NCC obtained by gravimetry or by impedance analysis using different formulas (indicated on the figure).

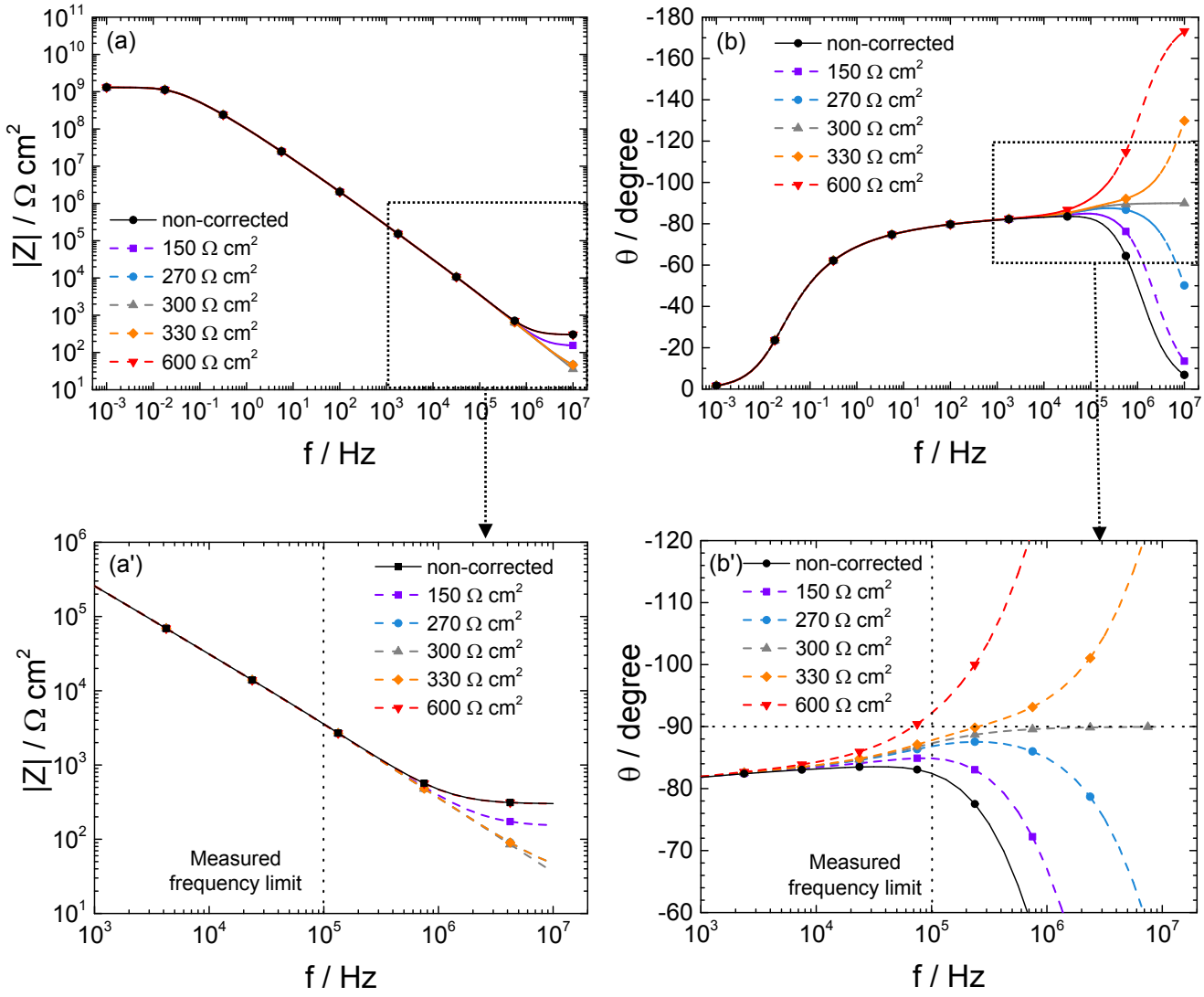

Fig. 1: Synthetic impedance calculated for a Young impedance, Eq. (6), in series with an electrolyte resistance, with: $\delta = 20$ µm, $\rho_0 = 10^{13}$ Ω cm, $\lambda = 1.3\ 10^{-4}$ cm, $\varepsilon_w = 10$, $R_e = 300$ Ω cm^2. The uncorrected curves and curves corrected with different R_e values indicated on the figure are shown. Parts (a') and (b') are expanded views of parts (a) and (b), relevant to the high frequency region.

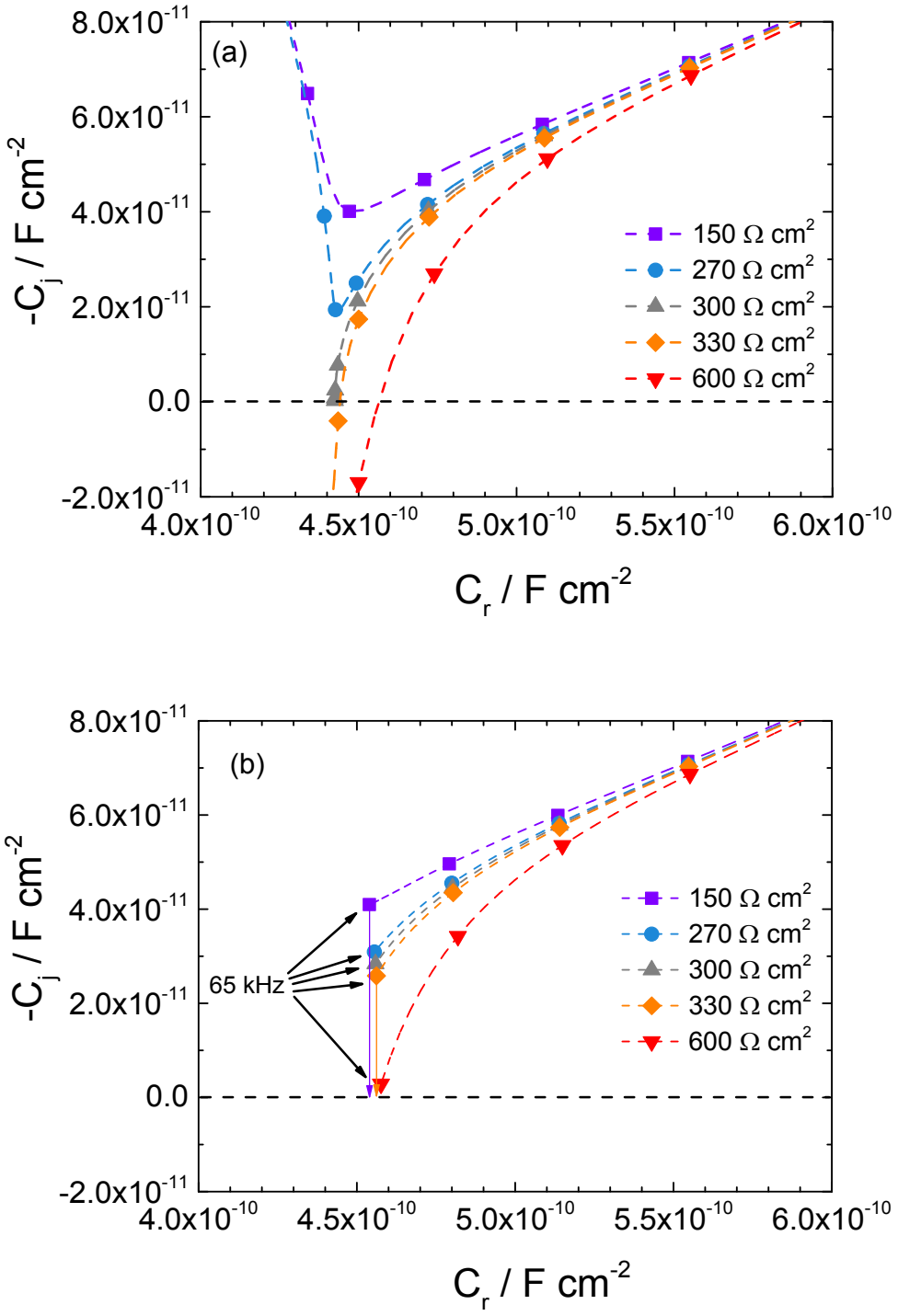

Fig. 2: Influence of the R_e value used for the conversion of the calculated impedance shown in Fig. 1 to capacitance. Complex-capacitance plots are shown for the R_e values indicated on the figure. (a) high frequency region and (b) same curves truncated at 65 kHz (measured frequency limit in this work)

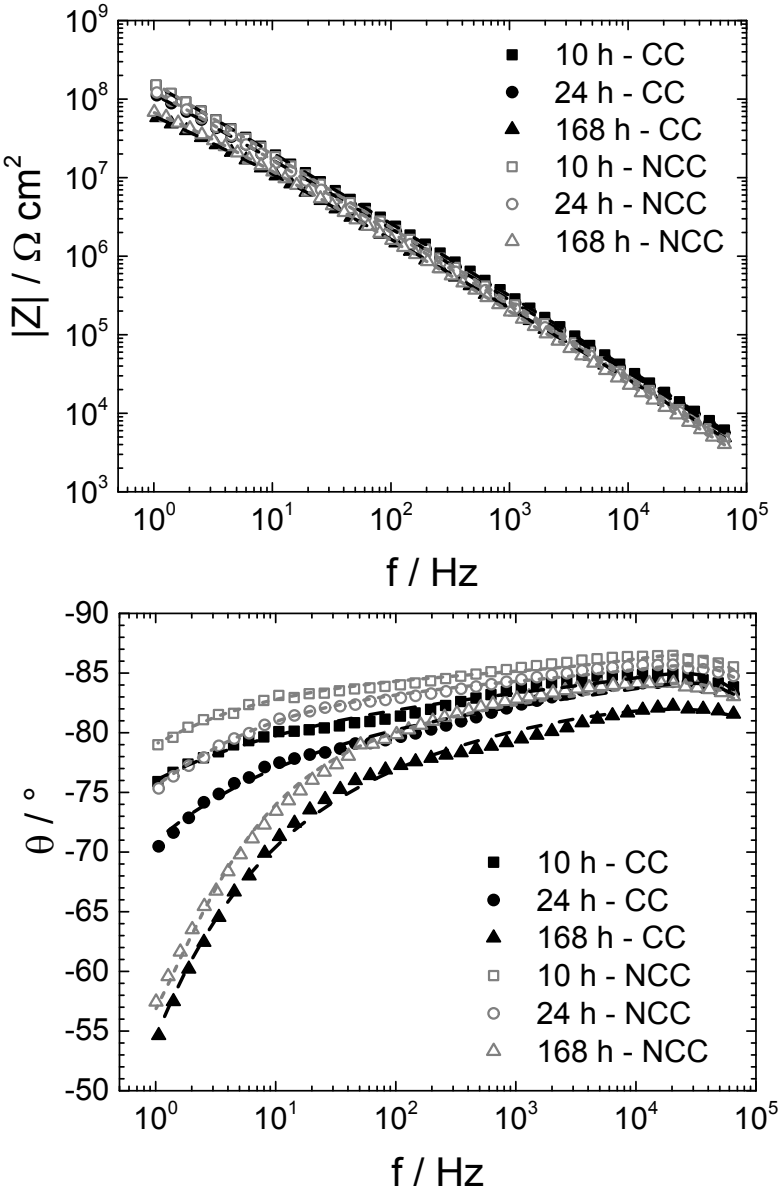

Fig. 3: Impedance responses in Bode format for the AA2024 coated samples (CC and NCC) after 10 h, 24 h and 168 h of immersion in 0.5 M NaCl solution. The solid lines are the best fitted curves according to Eq. (7).

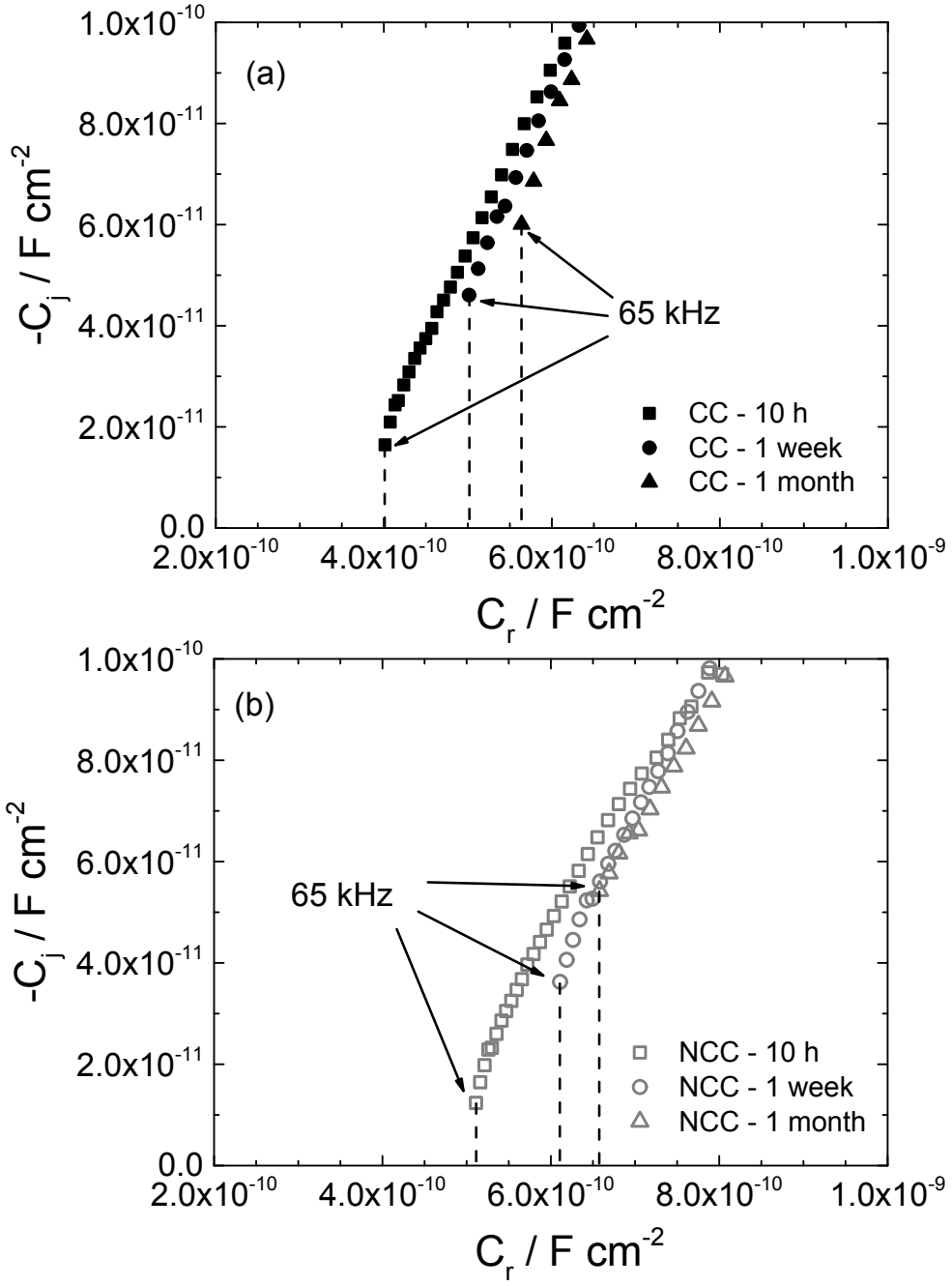

Fig. 4: Complex-capacitance plots corresponding to EIS spectra of CC and NCC obtained after 10 h, 1 week and 1 month of immersion in 0.5 M NaCl solution. The axis are not orthonormal to make the extrapolation to the C_r axis better visible.

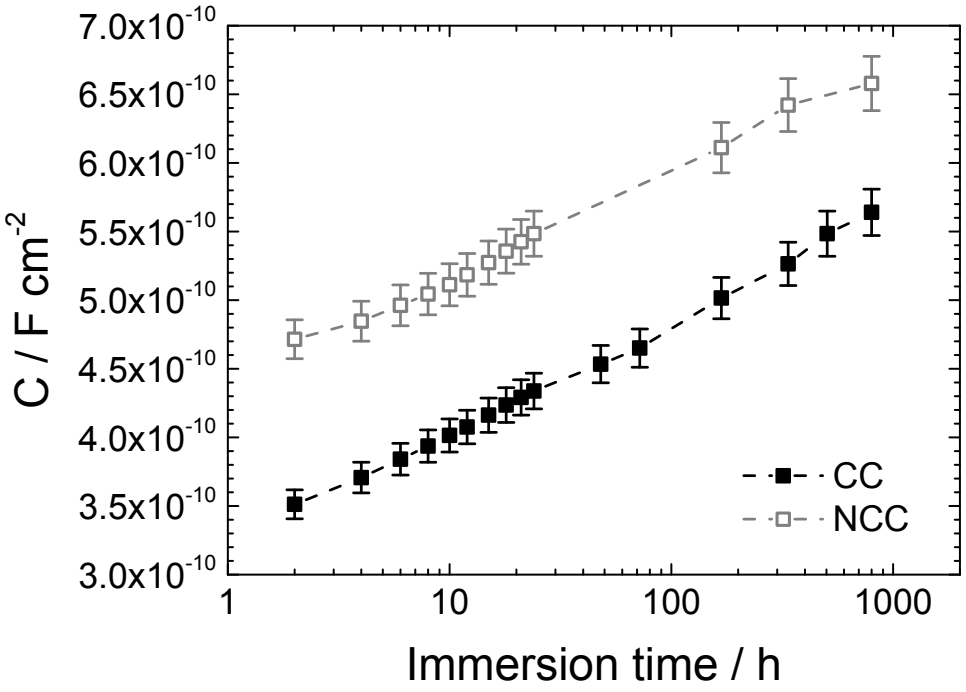

Fig. 5: Variation of the capacitance obtained from the complex-capacitance plots (at 65 kHz) for CC and NCC as a function of immersion time in 0.5 M NaCl.

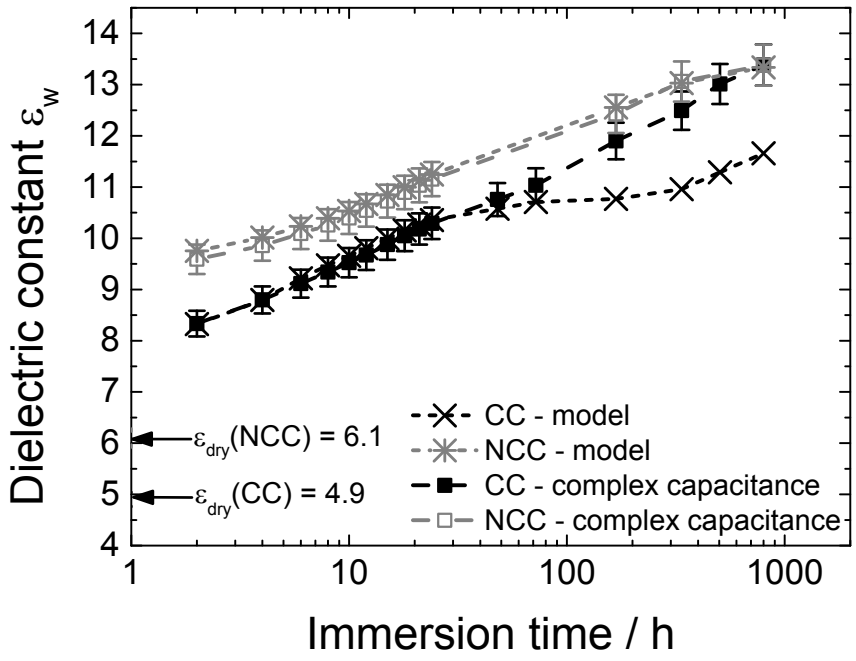

Fig. 6: Comparison of the wet dielectric constant (ε_w) obtained from the impedance data analysis (in the frequency range 65 kHz to 1 Hz) and from the complex-capacitance plots at 65 kHz.

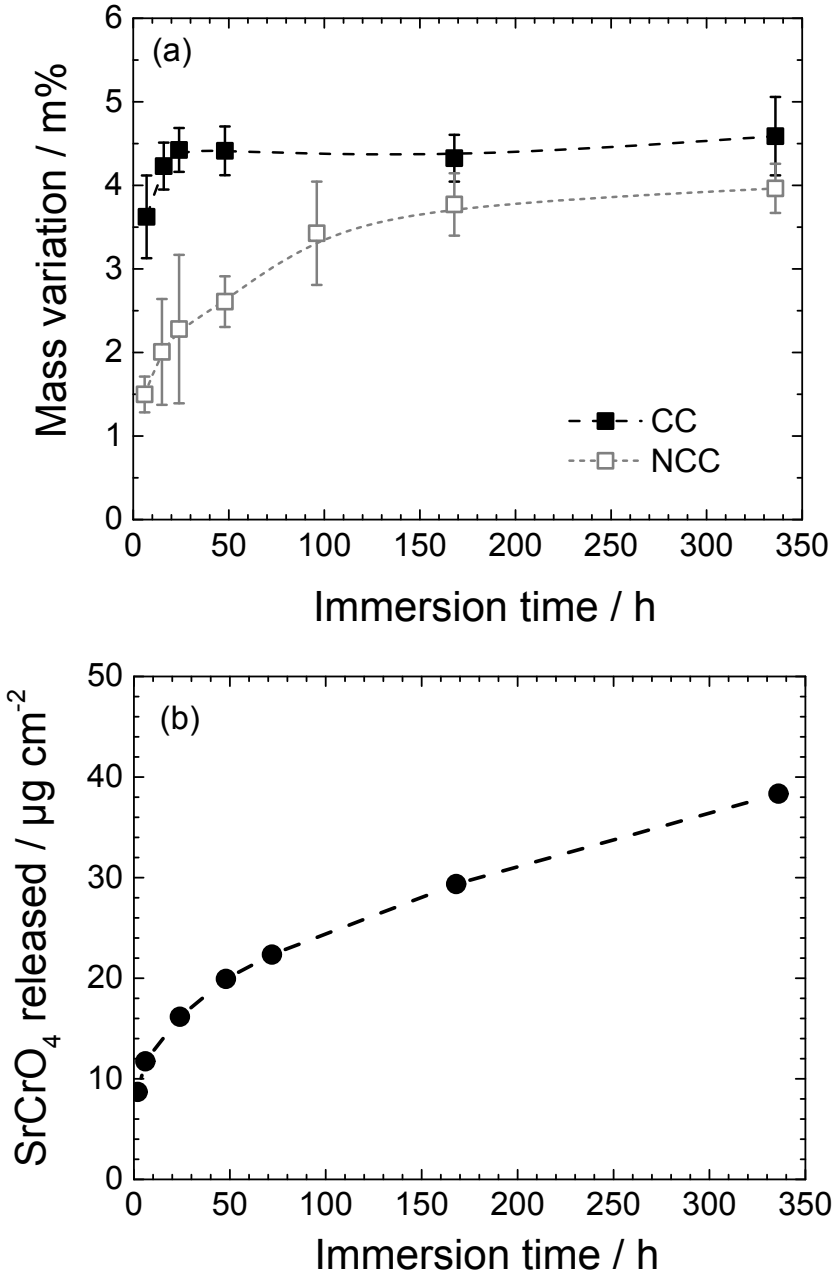

Fig. 7: (a) Percent mass variation (m %) vs. immersion time in 0.5 M NaCl for CC and NCC (supported coatings on a thin Al foil) obtained from gravimetric method at room temperature. Error bars account from at least five independent measurements.
(b) Immersion time dependence of the amount of $SrCrO_4$ released from a CC sample in contact with a 0.5 M NaCl solution.

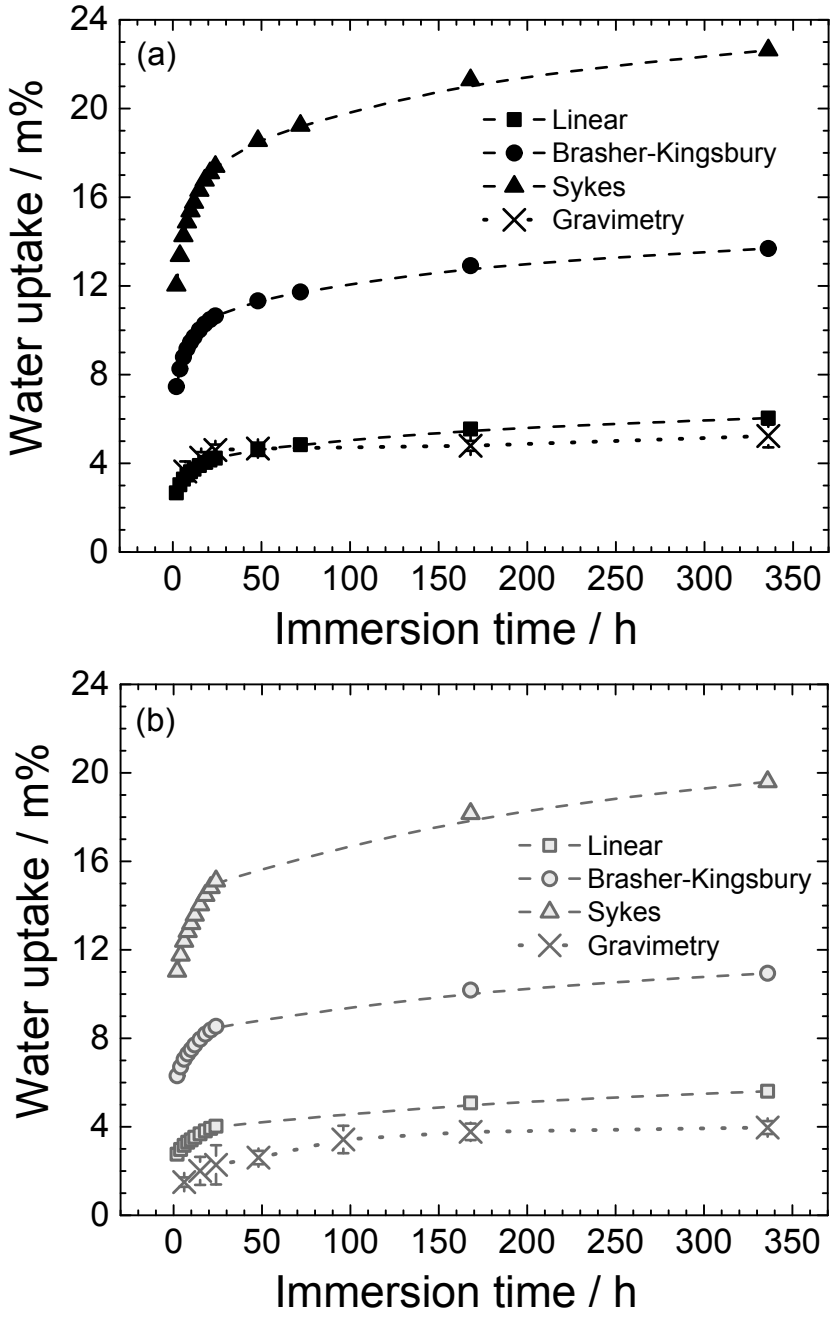

Fig. 8: Comparison of the water uptake (m %) for (a) CC and (b) NCC obtained by gravimetry or by impedance analysis using different formulas (indicated on the figure).